

Spin Hall Effect of Excitons

Shun-ichi Kuga,¹ Shuichi Murakami,^{2,3,*} and Naoto Nagaosa^{1,4}

¹*Department of Applied Physics, University of Tokyo,
7-3-1 Hongo, Bunkyo-ku, Tokyo 113-8656, Japan*

²*Department of Physics, Tokyo Institute of Technology,
2-12-1 Ookayama, Meguro-ku, Tokyo 152-8551, Japan*

³*PRESTO, Japan Science and Technology Corporation (JST), Saitama, 332-0012, Japan*

⁴*Cross-Correlated Materials Research Group (CMRG), ASI, RIKEN, Wako 351-0198, Japan*

Spin Hall effect for excitons in alkali halides and in Cu₂O is investigated theoretically. In both systems, the spin Hall effect results from the Berry curvature in k space, which becomes nonzero due to lifting of degeneracies of the exciton states by exchange coupling. The trajectory of the excitons can be directly seen as spatial dependence of the circularly polarized light emitted from the excitons. It enables us to observe the spin Hall effect directly in the real space-time.

PACS numbers: 71.35.-y, 72.25.Dc, 85.75.-d

I. INTRODUCTION

Spin Hall effect (SHE) is attracting interest recently because it can produce spin current without magnetism or magnetic field. The research was triggered by the two theoretical proposals on the intrinsic mechanism on the SHE^{1,2}, and it has been intensively studied both theoretically and experimentally. There are various experiments on the SHE in doped semiconductors and in metals^{3,4,5,6} by optical and electrical methods. In these observations in electronic systems, the spin current is seen as an effect summed over many electrons, while the motion of the individual electrons cannot be seen. Therefore, comparison between theory and experiments is sometimes indirect and not straightforward. An experimental method to see directly the electron trajectory is highly desired. At first sight it seems impossible because condensed materials have a huge number of electrons, which cannot be distinguished from each other.

Apart from electronic systems, we have one example where one can observe directly the SHE as a trajectory of the particle: light⁷. As the intrinsic SHE is induced by the Berry phase, it is not limited to electronic systems but also seen in other (even classical) wave phenomena such as light. In this SHE of light, the difference of the refractive indices at an interface of two different media plays the role of the “electric field” in the electronic SHE. The SHE of light at the interface is recently measured in a high accuracy of about 1Å using weak measurement⁸.

In this letter we theoretically propose a way to optically observe the trajectory of an elementary excitation driven by the SHE. We consider two candidates; transverse excitons in alkali halides and orthoexcitons in Cu₂O. We propose an experimental setup, and estimate the shift size due to the SHE, which turns out to be enough magnitude for observation. In both systems, an electron-hole exchange coupling lifts the degeneracy of the excitonic states, which gives rise to the Berry curvature in k space of the center-of-mass motion. It leads to the SHE, namely spin-dependent trajectory of the excitons. After the radiative lifetime, these excitons emit

light, whose circular polarization is determined by the exciton spins. Thus by spatially resolving the circular polarization of the emitted light, we can see how the excitons move in real space in a spin-dependent way. It is the first proposal of a real-space observation of the Berry-phase-driven SHE in electronic systems.

II. SPIN HALL EFFECT OF EXCITONS IN ALKALI HALIDES

Due to the spin-orbit coupling, exciton states in alkali halides with the lowest energy consists of an electron in the Γ_6^+ conduction band, and a hole in the Γ_8^- valence band, and these states are further classified into pure spin-triplet states (total angular momentum $J = 2$) and spin singlet-triplet mixed states ($J = 1$). Exchange interaction and the spin-orbit coupling lifts the degeneracy among these states⁹, and the energies of the $J = 2$ excitons are lower than those of the $J = 1$ due to the analytic exchange interaction. The $J = 1$ excitons are allowed for optical dipolar transition, and are suitable for real-space imaging of the SHE. Meanwhile, the $J = 2$ states are dipolar forbidden. Hence we restrict ourselves to the $J = 1$ excitons. The nonanalytic exchange Hamiltonian with the basis $\{|O_x\rangle, |O_y\rangle, |O_z\rangle\}$ within the $J = 1$ states is given by¹⁰

$$H_{ex}(\vec{K}) = \frac{\Delta_{LT}}{K^2} (K^2 - (\vec{K} \cdot \vec{S})^2), \quad (1)$$

where \vec{S} is the set of the spin-1 matrices. Δ_{LT} is the longitudinal-transverse (L-T) splitting, which can be experimentally determined e.g. from polarization beating of the emission¹¹. We neglect higher order terms in \vec{K} . In addition, for simplicity, we assume that the analytic exchange (the splitting between $J = 1$ and $J = 2$) is much larger than the nonanalytic one Δ_{LT} . In the calculation of the Berry curvature, this assumption allows us to retain only the matrix elements within the $J = 1$ states among the various matrix elements in the 8×8 Hamiltonian in the space spanned by $J = 1$ and $J = 2$ states (see

Ref. 10 and Table 8 in Ref. 12). This Hamiltonian H_{ex} is diagonalized by eigenstates of the helicity $\lambda = (\vec{K} \cdot \vec{S})/K$ with eigenvalues of $\lambda = \pm 1, 0$. Hence, the eigenstates of $H_{ex}(\vec{K})$ are twofold degenerate transverse modes and a longitudinal mode, whose energies differ by Δ_{LT} . This L-T splitting gives rise to the Berry curvature for the $J = 1$ excitons, leading to the SHE.

When the eigenstates are degenerate, a wavepacket follows the semiclassical equations of motion^{1,13,14,15}:

$$\dot{\vec{R}}_c = \frac{1}{\hbar} \frac{\partial \varepsilon_n(\vec{K}_c)}{\partial \vec{K}_c} + \dot{\vec{K}}_c \times \eta^\dagger \vec{\mathcal{F}}_n(\vec{K}_c) \eta, \quad (2)$$

$$\hbar \dot{\vec{K}}_c = -\frac{\partial V(\vec{R}_c)}{\partial \vec{R}_c}, \quad \dot{\eta} = -i \dot{\vec{K}}_c \cdot \vec{\mathcal{A}}_n(\vec{K}_c) \eta, \quad (3)$$

where \vec{R}_c, \vec{K}_c are the center position and the wavevector of the wavepacket, $\varepsilon_n(\vec{K}_c)$ is the energy dispersion of the n -th band, $V(\vec{R}_c)$ is an external potential, and $\eta = (\eta_1, \eta_2)$ is the internal degree of freedom of the two degenerate transverse exciton bands. $\vec{\mathcal{A}}_n(\vec{K})$ and $\vec{\mathcal{F}}_n(\vec{K}_c)$ are Berry connection and Berry curvature, which are defined as

$$\begin{cases} [\mathcal{A}_n^\mu(\vec{K})]_{ij} \equiv -i \langle n_i(\vec{K}) | \frac{\partial}{\partial K_\mu} | n_j(\vec{K}) \rangle, \\ \mathcal{F}_n^\rho(\vec{K}) \equiv \epsilon_{\mu\nu\rho} \left(\frac{\partial \mathcal{A}_n^\nu(\vec{K})}{\partial K_\mu} + i \mathcal{A}_n^\mu(\vec{K}) \mathcal{A}_n^\nu(\vec{K}) \right), \end{cases} \quad (4)$$

where $|n_i(\vec{K})\rangle$ is an eigenstate of the n -th band and i is the label for each eigenstate within the degenerate band. The term $\dot{\vec{K}} \times \eta^\dagger \vec{\mathcal{F}} \eta$ in the equation of motion for $\dot{\vec{R}}_c$ is called anomalous velocity, which leads to the SHE. The Berry phase changes sign when the spin direction is reversed. Therefore, two wavepackets with opposite spins move along opposite directions to each other. This mechanism is responsible for the SHE of electrons in p-type semiconductors¹ and that of light⁷.

The Berry curvature for the $J = 1$ exciton states can be calculated from H_{ex} in the same way as that in the SHE of light⁷, because the two cases share the same feature of L-T splitting in the spin-1 systems. Therefore the Berry curvature of the transverse states with helicity of $\lambda = \pm 1$ is then calculated as

$$\mathcal{F}_n^\rho(\vec{K}) = \lambda \frac{K_\rho}{K^3}. \quad (5)$$

The longitudinal state ($\lambda = 0$) has a vanishing Berry curvature, and it does not undergo a shift due to the SHE.

We propose an experiment to detect the SHE in the real space and evaluate the Hall shift. The SHE requires a nonzero $\dot{\vec{K}}_c$ as seen from Eq. (3). Namely, one should apply an external force to the exciton to see a shift due to the SHE. For electrons an electric field is sufficient, whereas an exciton cannot be accelerated by an electric

field. Instead, a local strain gives rise to a potential gradient and accelerates excitons, inducing the SHE. Thus we propose the following setup; we prepare a transverse exciton wavepacket with momentum along the z direction, and apply a uniaxial local strain, so that the excitons feel a force along the x direction, as shown in Fig.1.

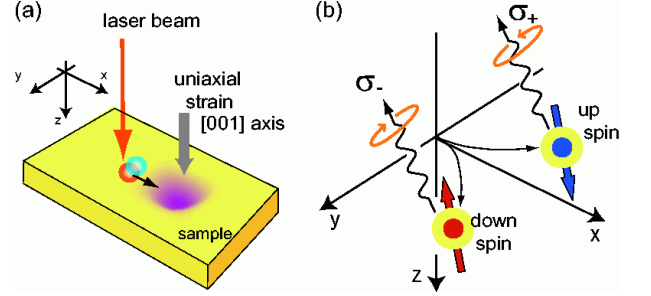


FIG. 1: (a) Experimental setup for the detection of SHE in alkali halides. The twofold degenerate wavepacket of the transverse excitons moves toward the center of the uniaxial trapping potential, along the x direction. (b) Schematic figure of the spin Hall effect of excitons. The up- and down-spin wavepackets are deflected to the $\mp y$ directions, respectively, and they emit light with opposite circular polarizations.

A strain-induced potential well has been developed for Cu_2O ¹⁶, but not for alkali halides to our knowledge. Therefore, we estimate the shift from existing data on alkali halides. From the data on the thin-film RbI for example, the effect of uniaxial strain is 25-45 meV for 1 kbar^{17,18,19}. Because the crystal is easily broken by high uniaxial pressure, we take a lower value for a trapping potential, 4meV for 0.1kbar as an example. We assume the size of the trap to be several hundred micrometers, as developed for Cu_2O ¹⁶. Thus we consider a $200\mu\text{m}$ -4meV configuration of the trapping potential. The force acting on the exciton wavepacket is $3.2 \times 10^{-18}\text{N}$, and the corresponding rate of the wavevector change is $\dot{K}_x \approx 3.0 \times 10^{16}\text{m}^{-1}\text{s}^{-1}$. When we take RbI for example, the typical wavenumber is $k_0 = 0.8 \times 10^6\text{cm}^{-1}$. The magnitude of the Berry curvature is $F^z = k_0^{-2} \approx 1.6 \times 10^{-16}\text{m}^2$. Therefore the anomalous velocity is $v_a = \dot{K}_x F^z \approx 4.8\text{m/s}$ and the shift is $y_a = v_a \tau \approx 8\text{nm}$, where $\tau = 1.7\text{ns}$ is the lifetime of the exciton in RbI, which is governed by self-trapping process²⁰. We note that this self-trapping instability can be reduced or avoided by choosing other materials such as III-V or II-VI compounds, AgBr, and TlBr, where the free state of exciton is more stable than the self-trapped state. In these materials, the shift of the excitons could be much longer²¹.

Because of the uncertainty principle, in order for the wavepacket to have a well-defined wavenumber, the size of the wavepacket in k space should be much larger than the wavenumber. Hence the ratio between the size of the exciton wavepacket and the transverse shift is small, and the direct observation of the SHE might be difficult. Nevertheless, a wavepacket deflected to the transverse direction is spin-polarized and emits a circularly polarized

light. Therefore, one can observe the SHE by detecting the spatial dependence of the circular polarization from the two wavepackets deflected in the opposite direction.

III. SPIN HALL EFFECT OF ORTHOEXCITON IN Cu_2O

In Cu_2O , the exciton states with the lowest energy, composed of the Γ_7^+ -valence band and the conduction band, is the $1S$ exciton. Because the valence band and the conduction band share the same parity, radiative recombination of the $1S$ exciton is dipolar forbidden, and therefore this state has a long radiative lifetime. The

four states in the $1S$ yellow excitons are classified into three Γ_5^+ orthoexciton states and one Γ_2^+ paraexciton state. The orthoexcitons are singlet-triplet mixed states, while the paraexciton is purely spin-triplet. Therefore exchange interaction exists only in the singlet states, and affects only the energy of the orthoexcitons, while the paraexcitons remain intact. The energy splitting between ortho and paraexcitons due to the exchange interaction is about 12meV. Furthermore, the degeneracy of the three orthoexciton states is lifted by (nonanalytic) exchange splitting. The matrix form of the exchange interaction among the orthoexciton states $\{|O_{yz}\rangle, |O_{zx}\rangle, |O_{xy}\rangle\}$ is given as

$$H_{ex}(\vec{K}) = \begin{bmatrix} \Delta_Q \frac{K_y^2 K_z^2}{K^2} + \Delta_3(3K_x^2 - K^2) & (\Delta_Q \frac{K_x^2}{K^2} + \Delta_5)K_x K_y & (\Delta_Q \frac{K_y^2}{K^2} + \Delta_5)K_z K_x \\ (\Delta_Q \frac{K_x^2}{K^2} + \Delta_5)K_x K_y & \Delta_Q \frac{K_x^2 K_z^2}{K^2} + \Delta_3(3K_y^2 - K^2) & (\Delta_Q \frac{K_x^2}{K^2} + \Delta_5)K_y K_z \\ (\Delta_Q \frac{K_y^2}{K^2} + \Delta_5)K_z K_x & (\Delta_Q \frac{K_x^2}{K^2} + \Delta_5)K_y K_z & \Delta_Q \frac{K_x^2 K_y^2}{K^2} + \Delta_3(3K_z^2 - K^2) \end{bmatrix}. \quad (6)$$

where the parameters are $\Delta_Q k_0^2 = 5.0\mu\text{eV}$, $\Delta_3 k_0^2 = -1.3\mu\text{eV}$, $\Delta_5 k_0^2 = 2.0\mu\text{eV}$ ²² with the wavenumber $k_0 \equiv 2.62 \times 10^7 \text{m}^{-1}$, as obtained experimentally from the high resolution spectroscopy of polaritons²².

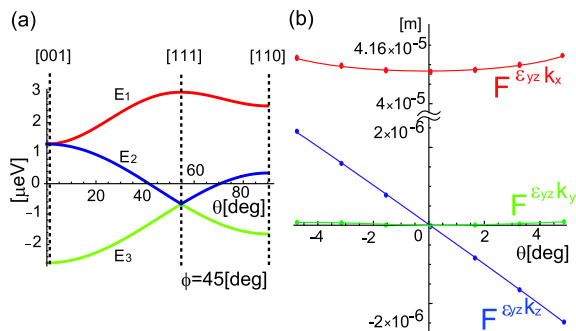


FIG. 2: (a) Energy dispersion of the exchange interaction and (b) distribution of the Berry curvature $F_n^{\epsilon\mu}$ in Cu_2O . They are shown as a function of the polar angle θ of \vec{K} , with the azimuthal angle $\phi = 45^\circ$. The strain ϵ_{yz} is set to be zero.

The wave-vector dependence of the exchange interaction (6) is illustrated in Fig. 2(a). The eigen energies $E_1(\vec{K})$ and $E_2(\vec{K})$ are degenerate along the $[001]$ direction and $E_2(\vec{K})$ and $E_3(\vec{K})$ are degenerate along the $[111]$ direction. One possible experiment is to make a potential trap exert a force to the exciton, as we considered in alkali halides. In Cu_2O , however, the strain is typically of the order of meV, much larger than the exchange coupling ($\sim \mu\text{eV}$). Hence one cannot ignore the strain in the calculation of the Berry curvature. This local strain in general reduces considerably the Berry cur-

vature stemming from the exchange coupling, because of its larger energy scale. To overcome this difficulty, we consider another type of strain: a shear strain $\epsilon \equiv \epsilon_{yz}$. The shear strain brings about an additional term to the Hamiltonian as $H'_{ij} = \Lambda \epsilon_{yz} (\delta_{i2} \delta_{j3} + \delta_{i3} \delta_{j2})$. For simplicity we change the normalization of the dimensionless strain parameter $\epsilon \equiv \epsilon_{yz}$, by taking $\Lambda = 8.1\text{meV}$ which is the energy shift expected for 5kbar shear strain, that is calculated from the data in¹⁶. Using this we consider a Berry curvature in the hyperspace of $\epsilon\text{-}\vec{K}$, which follows¹³

$$\dot{R}_\mu = \frac{1}{\hbar} \frac{\partial E_n}{\partial K_\mu} - \epsilon \eta^\dagger \mathcal{F}_n^{\epsilon\mu}(\vec{K}) \eta. \quad (7)$$

with Berry connection and Berry curvature that are defined as

$$[\mathcal{A}_n^\epsilon(\vec{K})]_{ij} \equiv -i \langle n_i(\vec{K}) | \frac{\partial}{\partial \epsilon} | n_j(\vec{K}) \rangle, \quad (8)$$

$$\mathcal{F}_n^{\epsilon\mu}(\vec{K}) \equiv \frac{\partial \mathcal{A}_n^\mu}{\partial \epsilon} - \frac{\partial \mathcal{A}_n^\epsilon}{\partial K_\mu} + i [\mathcal{A}_n^\epsilon, \mathcal{A}_n^\mu], \quad (9)$$

Because the Hamiltonian matrix $H_{ex} + H'$ is real, the eigenvectors can be chosen as real. The Berry curvature $\mathcal{F}^{\epsilon\mu}(\vec{K})$ is then pure imaginary and Hermitian. If the state considered is nondegenerate, the Berry curvature is scalar (1×1 matrix), and therefore it vanishes. On the other hand, when the state is twofold degenerate, as in $[001]$ or in $[111]$ direction, the Berry curvature is a 2×2 matrix. It is therefore proportional to the Pauli matrix σ_y :

$$\mathcal{F}^{\epsilon\mu}(\vec{K}) = F^{\epsilon\mu}(\vec{K}) \sigma_y. \quad (10)$$

Thus to see the SHE, the exciton states should be degenerate, which occurs along the high-symmetry lines. For

concreteness, we hereafter focus on the twofold degeneracy along the $[0, 0, 1]$ direction ($\vec{K} \parallel \hat{z}$) as the degenerate bands in the semiclassical equation of motion (3). Then the eigenstates $|n_1(\vec{K})\rangle$ and $|n_2(\vec{K})\rangle$ with eigenenergies $E_1(\vec{K})$ and $E_2(\vec{K})$ in Fig. 2(a) are considered as pseudospin states. Along the $[001]$ direction, these states become $|O_{yz}\rangle$ and $|O_{zx}\rangle$.

Figure 2(b) is the distribution of $F^{\epsilon\mu}$. We note that $F^{\epsilon\mu}$ depends on gauge, even though the anomalous velocity does not, and Fig. 2(b) is based on a particular gauge choice. The typical size of the Berry curvature is expected to be $F \sim (\Lambda/\Delta_{\text{gap}})k_0$ from consideration of relevant energy scales, where Δ_{gap} denotes the energy gap between the $(|n_1\rangle, |n_2\rangle)$ states and the $|n_3\rangle$ state. Because Λ and Δ_{gap} are of the order of meV and μeV , respectively, this estimate agrees with Fig. 2(b).

In fact, for $\vec{K} \parallel \hat{z}$ the Berry curvature can be calculated analytically as $\mathcal{F}^{ex}(\vec{K}) = (\Delta_5\Lambda)/(9\Delta_3k_0^3) = 4.06 \times 10^{-5}\text{m}$, and the other components are zero: $\mathcal{F}^{ey}(\vec{K}) = 0$, $\mathcal{F}^{ez}(\vec{K}) = 0$. The reason for the vanishing y and z components is the mirror symmetry with respect to the yz plane, and the twofold rotational symmetry around the z axis, respectively. Therefore, for \vec{K} along the $[001]$ direction, the anomalous velocity is along the x direction. Because the SU(2) Berry curvature $\mathcal{F}^\mu(\vec{K})$ is proportional to σ_y , we take the eigenvectors of σ_y , i.e. $\frac{1}{\sqrt{2}}\begin{pmatrix} 1 \\ \pm i \end{pmatrix}$ (in the $|n_1\rangle$ - $|n_2\rangle$ basis), and the semiclassical equations of motion (3) is diagonalized. In this basis, the spin η only acquires U(1) phase in time evolution, but does not change its direction. Therefore, for the wavenumber along the $[001]$ direction, the wavepackets for $(|O_{xz}\rangle \pm i|O_{yz}\rangle)/\sqrt{2}$ have opposite anomalous velocity, and their spins are along $\pm z$, respectively. These excitons emit circularly polarized light depending on its spin state²³. This enables us to see this spin Hall shift directly by an optical method.

The anomalous velocity is proportional to ϵ . Therefore, in order to induce the SHE, the strain should be varied externally. One may consider adding an oscillating strain with frequency ω . Then the typical size of the shift is $\epsilon(\Lambda/\Delta_{\text{gap}})/k_0 \sim (E_{\text{str.}}/\Delta_{\text{gap}})/k_0$, where $E_{\text{str.}} (\sim \Lambda\epsilon)$ is the energy shift of excitons by strain. Thus only the small strain of the order of μeV gives rise to the shift of the order of a wavenumber $\sim 600\text{nm}$. Although the radiative lifetime is $\tau_{\text{rad.}} \sim 14\mu\text{s}$ ²⁴, the lifetime of the orthoexcitons is much shorter: $\tau \sim 3\text{ns}$, due to a nonradiative rapid conversion from orthoexcitons to paraexcitons. The oscillation of the strain ϵ should be faster than $1/\tau$, i.e. be as fast as gigahertz in frequency.

The light emission from the orthoexciton may be reduced by several reasons. First, among all the orthoexcitons only the fraction of $\tau/\tau_{\text{rad.}} \sim 2 \times 10^{-4}$ emit light. The resolution to detect this emission is it to be well achievable, because the radiative decay rate of excitons has been measured in experiments²⁴. Furthermore, when the density of the orthoexcitons exceed a critical value ($\sim 10^{15}\text{cm}^{-3}$), the spin exchange process between two orthoexcitons will be effectively convert orthoexcitons into

paraexcitons in a short timescale ($\sim 100\text{ps}$)²⁵. A typical density of excitons by continuous wave (CW) laser is 10^{13} - 10^{14}cm^{-3} ; it is well below the critical density, and it is not a problem for the proposed experiment. The interaction between orthoexcitons also leads to phase decoherence, but it does not affect the SHE, as Eqs. (2)(3) remains unaffected. This situation is similar to the electrons in solids, where the mean free path is much shorter than the excitons, but still shows the spin Hall effect. This is because the spin Hall effect is the accumulative effect of the transverse motion of the particles, which does not require the coherence of the process.

IV. SUMMARY AND DISCUSSIONS

In conclusion, we theoretically investigate the SHE of the excitons in alkali halides and in Cu_2O . The exchange coupling lifts the threefold degeneracy of the orthoexcitons, while in some directions of the wavenumber double degeneracy remains. This remaining double degeneracy gives rise to nonzero SU(2) Berry curvature, leading to the SHE. This SHE can be observed as a position-dependent circularly polarized light emitted from the orthoexcitons.

Recently Yao and Niu²⁶ proposed SHE for excitons in GaAs quantum well. In their paper the main contribution to the Berry curvature comes from the heavy-hole light-hole mixing in the quantum well, whereas in the present paper the exchange coupling between the hole and electron spins is the main source of the Berry curvature. Because of the degeneracy of the energy spectrum, the Berry curvature is enhanced in our setup, thereby the SHE becomes prominent. Furthermore, we propose in this paper a realistic setup with target material specified. The proposed setup enables us to use modulation spectroscopy with high precision. This provides us with a space-time resolved measurement of the SHE.

As a closely related subject, an optical SHE has been observed in an exciton-polariton system²⁷, whose mechanism is totally different from the SHE in the present paper. The two different mechanisms for the intrinsic SHE are (A) precession due to the \mathbf{k} -dependent (Zeeman-like) field acting on the spin, and (B) the anomalous velocity from the \mathbf{k} -space Berry curvature. Although they are often confused with each other, they are distinct. The mechanism (A) is used in the optical SHE in exciton-polaritons^{27,28,29,30}, and in the SHE in the Rashba system². In these cases the spin-orbit coupling is linear in terms of the spin, which means that the spin-orbit splitting can be regarded as a ‘‘Zeeman-like’’ field, although the external magnetic field is zero. In these systems the mechanism (B) is absent because the contribution of the Berry curvature cancels between the two bands involved. On the other hand, the mechanism (B) causes the SHE in excitons in the present paper, as well as the SHE in the Luttinger model¹. This mechanism works even when the Hamiltonian is not linear in the spin

operator. This effect due to (B) is enhanced when band crossings exist near the Fermi energy, e.g. in the SHE in platinum³¹, while it is not the case in (A). Moreover, (B) gives an additional spin-dependent (anomalous) velocity and deflects the exciton trajectory, while (A) does not. Thus the mechanisms (A) and (B) are distinct, and the experiments proposed in the present paper allows us a first real-space observation of the Berry-curvature mechanism (B) in electronic systems.

Acknowledgments

We are grateful to K. Yoshioka and M. Kuwata-Gonokami for fruitful discussions. This research is partly supported by Grant-in-Aids under the grant numbers 16076205, 17105002, 19019004, 19048008, 19048015, and 19740177 from the Ministry of Education, Culture, Sports, Science and Technology of Japan.

-
- * Corresponding Author; Electronic address: murakami@stat.phys.titech.ac.jp
- ¹ S. Murakami, N. Nagaosa and S. C. Zhang, *Science* **301**, 1348 (2003).
 - ² J. Sinova *et al.*, *Phys. Rev. Lett.* **92**, 126603 (2004).
 - ³ Y. K. Kato, R. C. Myers, A. C. Gossard and D. D. Awschalom, *Science* **306**, 1910 (2004).
 - ⁴ J. Wunderlich, B. Kaestner, J. Sinova and T. Jungwirth, *Phys. Rev. Lett.* **94**, 047204 (2005).
 - ⁵ E. Saitoh, M. Ueda, H. Miyajima and G. Tatara, *Appl. Phys. Lett.* **88**, 182509 (2006).
 - ⁶ S. O. Valenzuela and M. Tinkham, *Nature* **442**, 176 (2006).
 - ⁷ M. Onoda, S. Murakami and N. Nagaosa, *Phys. Rev. Lett.* **93**, 083901 (2004).
 - ⁸ O. Hosten and P. Kwiat, *Science* **319**, 787 (2008).
 - ⁹ Y. Onodera and Y. Toyozawa, *J. Phys. Soc. Jpn.* **22**, 833 (1967).
 - ¹⁰ K. Cho, *Phys. Rev. B* **14**, 4463 (1976).
 - ¹¹ W. Langbein, I. Shelykh, D. Solnyshkov, G. Malpuech, Yu. Rubo, and A. Kavokin, *Phys. Rev. B* **75**, 075323 (2007).
 - ¹² B. Hönerlage, R. Lévy, J. B. Grun, C. Klingshirn and, K. Bohne, *Phys. Rep.* **124**, 161 (1985).
 - ¹³ G. Sundaram and Q. Niu, *Phys. Rev. B* **59**, 14915(1999).
 - ¹⁴ R. Shindou, and K. Imura, *Nucl. Phys. B* **720**, 399 (2005).
 - ¹⁵ D. Culcer, Y. Yao and Q. Niu, *Phys. Rev. B* **72**, 085110 (2005).
 - ¹⁶ N. Naka and N. Nagasawa, *Phys. Rev. B* **70**, 155205 (2004).
 - ¹⁷ M. Itoh, S. Hashimoto and N. Ohno, *J. Phys. Soc. Jpn.* **59**, 1881(1990).
 - ¹⁸ H. Nishimura, K. Kitano, S. Kawase, and M. Nakayama, *Phys. Rev. B* **57**, 2592 (1998).
 - ¹⁹ N. Ohno, S. Hashimoto, M. Ito, *J. Phys. Soc. Jpn.* **59**, 361 (1990).
 - ²⁰ T. Tsujibayashi, K. Toyoda and T. Hayashi, *Solid State Commun.* **105**, 681 (1998).
 - ²¹ M. Ueda, H. Kanzaki, K. Kobayashi, Y. Toyozawa, and E. Hanamura, *Excitonic Processes in Solids*, Chap.4 (Springer-Verlag, 1986).
 - ²² G. Dasbach, D. Fröhlich, H. Stolz, R. Klieber, D. Suter, and M. Bayer, *Phys. Rev. Lett.* **91**, 107401 (2003); G. Dasbach, D. Fröhlich, R. Klieber, D. Suter, M. Bayer, and H. Stolz, *Phys. Rev. B* **70**, 045206 (2004).
 - ²³ R. J. Elliott, *Phys. Rev.* **124**, 340 (1961).
 - ²⁴ K. E. O'Hara, J. R. Gullingsrud and J. P. Wolfe, *Phys. Rev. B* **60**, 10872 (1999).
 - ²⁵ M. Kubouchi, K. Yoshioka, R. Shimano, A. Mysyrowicz, and M. Kuwata-Gonokami, *Phys. Rev. Lett.* **94**, 016403 (2005).
 - ²⁶ W. Yao and Q. Niu, *Phys. Rev. Lett.* **101**, 106401 (2008).
 - ²⁷ C. Leyder, M. Romanelli, J. Ph. Karr, E. Giacobino, T. C. H. Liew, M. M. Glazov, A. V. Kavokin, G. Malpuech and A. Bramati, *Nature Phys.* **3**, 628 (2007).
 - ²⁸ A. Kavokin, G. Malpuech, and M. Glazov, *Phys. Rev. Lett.* **95**, 136601 (2005).
 - ²⁹ M. Glazov, A. Kavokin, *J. Lumin.* **125**, 118 (2007).
 - ³⁰ M. M. Glazov and L. E. Golub *Phys. Rev. B* **77**, 165341 (2008).
 - ³¹ G.-Y. Guo, S. Murakami, T.-W. Chen and N. Nagaosa, *Phys. Rev. Lett.* **100**, 096401 (2008).